RESEARCH PAPER

# Synthesis and Pharmacological Screening of New Thiazolopyrimidines with Broad-Spectrum Bioactivity

**Archana R Patil[1], Basappa C Yallur[1*], Vishwa B Das[2], Mahesh Akki[3], Delicia A. Barretto[4], Ashwini Prabhu[5], Vinuta Kamat[6*]**

[1]Department of Chemistry, M. S. Ramaiah Institute of Technology (Affiliated to VTU, Belagavi), Bangalore-560054, Karnataka, India.
[2]Department of Chemistry, Mangalore University, Mangaluru-274199, Karnataka, India.
[3]Department of Chemistry, Smt. Kamala and Sri Venkappa M. Agadi College of Engineering and Technology, Lakshmeshwar-582116, Karnataka, India.
[4]School of Chemical Sciences, Goa University, Taleigao plateau, Panaji-403206, Goa, India.
[5]Division of Cell and Molecular Biology, Central Research Laboratory, Srinivas University, Mangalore 574146, India
[6]Department of Chemistry, Dayananda Sagar College of Engineering, Bangalore-560078, Karnataka, India.
***Corresponding Author**
**Email:** yallurbc@gmail.com, vinutakamat24@gmail.com
**Received:** 25th May, 2026; **Revised:** 6th June, 2026; **Accepted:** 20th Aug, 2026; **Available Online:** 27th Aug, 2026

***ABSTRACT***
Thiazolopyrimidine-6-carboxylate and thiazole-pyrimidine-6-carbonitrile derivatives were prepared using Biginelli reaction under solvent-free conditions. A series of synthesized compounds were characterized by FTIR, $^{1}$H-NMR, LC-MS, and $^{13}$C-NMR spectroscopy. Biological activity studies have been carried out for antioxidant, antibacterial, antidiabetic, anti-inflammatory, and anticancer studies for derivatives. Compounds **4a** and **2b** showed strong antibacterial activity against S. aureus, S. pyogenes, S. typhi, and P. aeruginosa, comparable to streptomycin. Compound **4a** was most effective among all tested compounds. Compounds **4a** ($IC_{50}$ = 36.43 µM), **4e** ($IC_{50}$ = 37.37 µM), and **2b** ($IC_{50}$ = 38.72 µM) showed strong antioxidant activity in DPPH assay. Their activity was comparable to standard ($IC_{50}$ = 37.37 µM), with compound **4a** being most potent. Compounds **4a** ($IC_{50}$ = 30.36 µM), **4e** ($IC_{50}$ = 30.69 µM), and **2b** ($IC_{50}$ = 31.81 µM) exhibited strong anti-inflammatory activity, comparable to standard ($IC_{50}$ = 31.03 µM). Compound **4a** was most potent among all synthesized derivatives. Compound **4e** ($IC_{50}$ = 39.62 µM) showed highest α-amylase inhibitory activity, comparable to standard ($IC_{50}$ = 40.83 µM). Other 4-series compounds like **4b** and **4c** also showed good antidiabetic potential. Compound **4e** ($IC_{50}$ = 29.94 µM) showed the strongest α-glucosidase inhibition, comparable to the standard ($IC_{50}$ = 30.40 µM). Other 4-series compounds like **4b** and **4c** also exhibited good antidiabetic activity. The compounds (**2b** and **4a**) exerted potential anticancer activity on glioma cells ($IC_{50}$ = 55.81 and 52.41 µg/mL), lung cancer ($IC_{50}$ = 45.01 and 39.81 µg/mL), and breast cancer ($IC_{50}$ = 50.5 and 34.38 µg/mL) cells.
**KEYWORDS:** Thiazolopyrimidine, antibacterial, anti-inflammatory, antioxidant, antidiabetic, anticancer.
**How to cite this article:** Patil AR, Yallur BC, Das VB, Akki M, Barretto DA, Prabhu A, Kamat V. Synthesis and pharmacological screening of new thiazolopyrimidines with broad-spectrum bioactivity. Int J Drug Deliv Technol. 2026;16(79s): 119-138. DOI: 10.25258/ijddt.16.79s.14
**Source of support:** Nil.
**Conflict of interest:** Nil.
**Graphical abstract:**

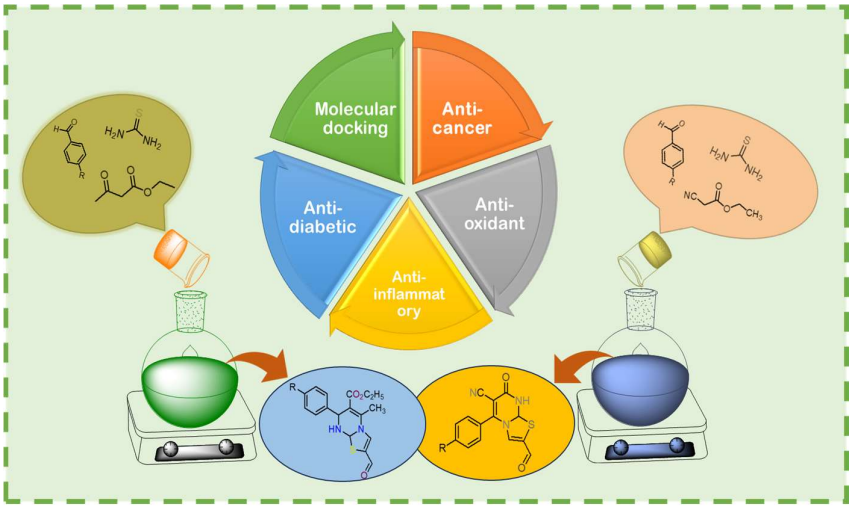


## INTRODUCTION

One of the significant classes of heterocyclic compounds is thiazolopyrimidines, which have attracted significant interest due to their diverse biological activities[1]. These substances have a special structure that combines the pyrimidine and thiazole rings, giving them a variety of therapeutic benefits, including antibacterial,[2] antiviral,[3] anti-inflammatory,[4] and anticancer[5, 6]. A lot of research has been done on their synthesis and functions due to their structural diversity and potential medical uses.[7] There are different ways to synthesize thiazolopyrimidines, and scientists continue to improve these methods to make them more effective.[8] The combination of thiazole and pyrimidine structures in these compounds plays an important role in their biological effects, as similar structures are found in many natural and medicinal molecules.[9] Thiazole derivatives are important because they have been used as anti-inflammatory drugs.[10, 11] Since both thiazole and pyrimidine are known for their ability to reduce inflammation and pain, combining them may enhance their effects.[12, 13] This idea has led to the development of thiazolopyrimidine compounds, which have been studied for their medicinal properties.[14, 15] Thiazolopyrimidines are structurally similar to purines and have shown strong anti-inflammatory activity, comparable to some commonly used drugs, but with little to no risk of causing stomach ulcers.[16, 17 18] Thiazolopyrimidine is a fascinating chemical structure that is similar to 5-fluorouracil (5-FU), a well-known cancer-fighting drug.[19] These compounds have been found to have many beneficial effects, including fighting bacteria [20], reducing inflammation [21], and treating conditions like Parkinson's disease and HIV.[22] They also show promise in treating cancer.[23] Additionally, thiazolopyrimidines can interact with certain body receptors (such as TRPV1), act as antioxidants [24], work as pesticides, inhibit specific enzymes like phosphatases and acetylcholinesterase, and help fight infections.[25]

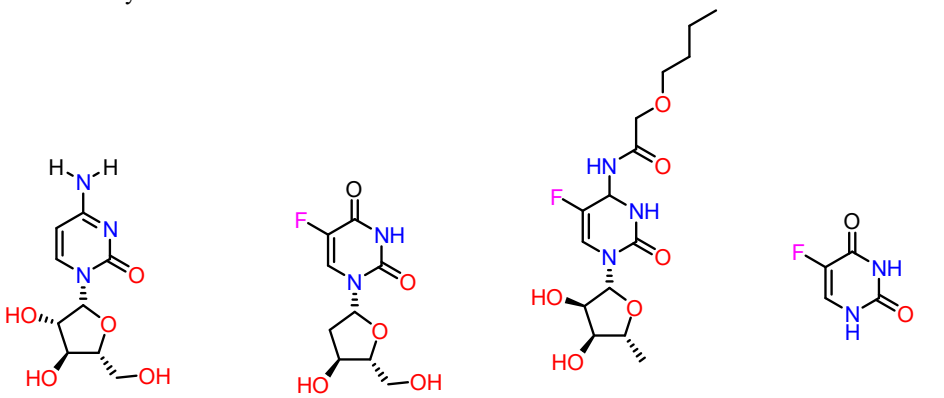


**Figure 1.** Pyrimidine analogues, used in chemotherapy to treat various cancer

It should be mentioned that several structural analogues of thiazolo- and oxazolo[3,2-*a*]pyrimidinones, like the antipsychotics Ritanserin and Setoperone, are employed in clinical treatment.[26]


**Figure 2.** Examples of thiazolo-[3,2-*a*]pyrimidinone structural analogues used in clinical medicine.

In this research work, we synthesized two different series of thiazolo[3,2-*a*]pyrimidine derivatives using two synthetic approaches, as these derivatives are known for their wide range of biological activities. The prepared novel derivatives were initially tested for their anti-inflammatory, anti-diabetic, and antioxidant properties. Based on these evaluations,

the compounds demonstrating the most significant activities were selected for an anticancer study. By studying these compounds, we aim to discover new potential drugs that may be beneficial in clinical applications.

## 2 RESULTS AND DISCUSSION

### 2.1 Chemistry

A mixture of aldehyde derivatives (1.0 mmol), thiourea (1.5 mmol), and ethyl acetoacetate was heated at 70 °C without a solvent in the presence of formic acid (10 mL). The reaction was monitored using thin-layer chromatography (TLC). Once completed, the mixture was cooled, and cold water was added. The product that formed was filtered and then recrystallized from ethanol to obtain pure compounds (**1a-d**). Next, the synthesized compounds (**1a-d**) were mixed with 2-bromomalonaldehyde and stirred in acetone at room temperature for about 16 hours. After removing the excess solvent, ice cubes were added, and the mixture was neutralized with sodium bicarbonate. The solid product was filtered and recrystallized from ethanol to obtain pure compounds (**2a-d**).

The newly produced compounds were confirmed using FTIR, $^{1}$H NMR, $^{13}$C NMR, and LC-MS techniques. For this compound (**2c**), the FTIR spectrum showed a peak at 2990 cm$^{-1}$ for C–H stretching and a strong peak at 1698 cm$^{-1}$ for the C=O group. Peaks at 1668 and 1242 cm$^{-1}$ indicated the presence of C=N and C–O (from methoxy group), respectively. In the $^{1}$H NMR spectrum, a singlet at $\delta$ 9.61 ppm corresponded to the aldehyde proton (–CHO), and a singlet at $\delta$ 3.37 ppm confirmed the presence of a methoxy group (–$OCH_3$). Aromatic and thiazole protons appeared between $\delta$ 8.32 and 6.92 ppm. The $^{13}$C NMR spectrum showed the aldehyde carbon at $\delta$ 182.5 ppm and the methoxy carbon at $\delta$ 55.6 ppm. Other carbon signals were also observed in expected regions. The LC-MS showed a molecular ion peak at m/z 359.97 [M+H], confirming the compound's molecular weight. The spectroscopic data of other compounds also matched well with their structures.

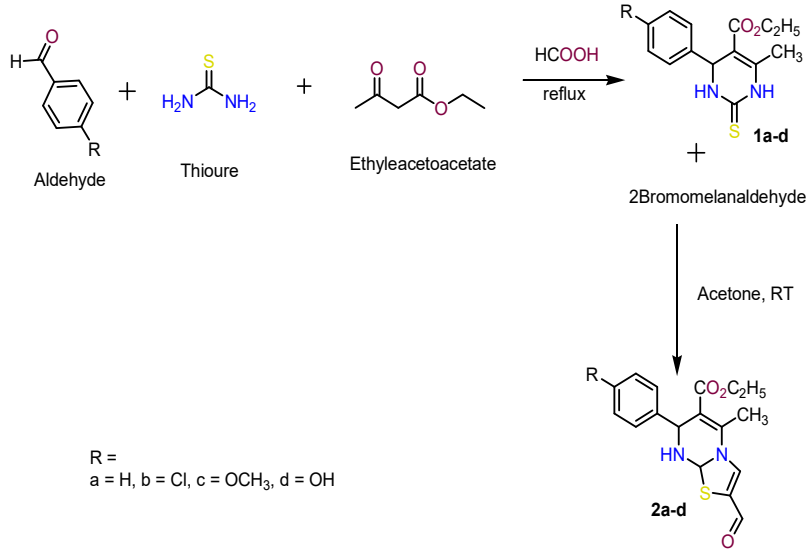


**Scheme 1**. Synthesis of thiazole pyrimidine-6-carboxylate derivatives

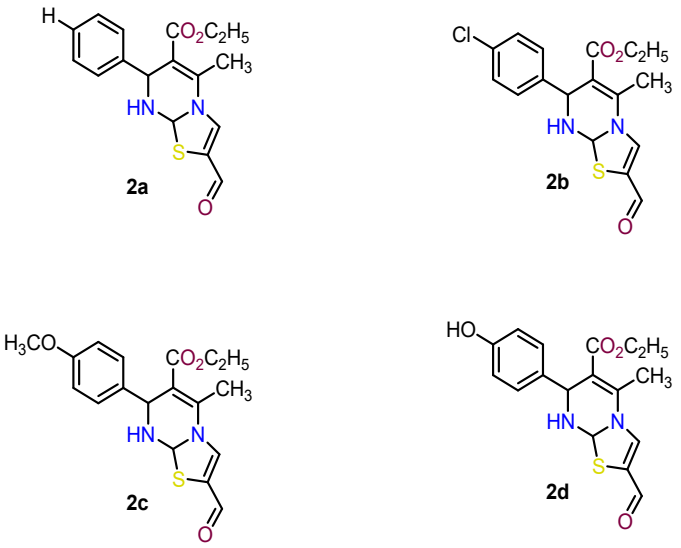


Synthesized thiazole pyrimidine-6-carboxylate derivatives

**3.1.2. Synthesis of thiazole pyrimidine-6-carbonitrile derivatives (4a-e)**

A mixture of the selected substituted benzaldehyde (0.01 mol), ethyl cyanoacetate (0.01 mol), thiourea (0.01 mol), and sodium carbonate (0.01 mol) was refluxed in 30 mL of ethanol for 6 hours. After cooling, the resulting solid was collected by filtration, washed with ether, and dried. The solid was then dissolved in 20 mL of water by heating at 80-90 °C until a clear solution was obtained. After cooling, acetic acid was added to acidify the solution, and stirring continued for 30 minutes. The resulting precipitate was filtered, washed with cold water, dried, and recrystallized from ethanol. Next, the synthesized product was mixed with 2-bromo-malonaldehyde and stirred in acetone at room temperature for about 16 hours. After removing the excess solvent, ice cubes were added, and the mixture was neutralized with sodium bicarbonate. The solid product was filtered and recrystallized from ethanol to obtain the pure compounds.

Compounds were confirmed using FTIR, $^{1}$H NMR, $^{13}$C NMR, and LC-MS. The FTIR spectrum showed a strong band at 2225 cm$^{-1}$ indicating the presence of a nitrile (–C≡N) group and a peak at 1680 cm$^{-1}$ for the carbonyl (C=O) group. In the $^{1}$H NMR spectrum (DMSO-$d_6$, 400 MHz), a singlet at $\delta$ 10.05 ppm confirmed the aldehyde proton (-CHO), a singlet at $\delta$ 8.7 ppm was assigned to the NH proton, a doublet at $\delta$ 8.07 ppm was due to aromatic proton, and a singlet at $\delta$ 5.40 ppm indicated the thiazole proton. The $^{13}$C NMR (100 MHz, DMSO-$d_6$) showed a signal at $\delta$ 180.8 ppm for the aldehyde carbon and other peaks in the expected regions. The LC-MS showed a molecular ion peak at m/z 284.34 [M]$^{+}$, confirming the molecular weight. Compound **4c** (Yield: 81%; mp:186-188 °C) showed FTIR bands at 2215 cm$^{-1}$ (–C≡N) and 1685 cm$^{-1}$ (C=O), indicating the presence of nitrile and aldehyde groups. In the $^{1}$H NMR (DMSO-$d_6$, 400 MHz), a singlet at $\delta$ 10.09 ppm was observed for the aldehyde proton, and a singlet at $\delta$ 9.24 ppm for the N-H proton. A triplet at $\delta$ 8.03 ppm and a multiplet at $\delta$ 8.18 ppm corresponded to aromatic protons. A singlet at $\delta$ 3.87 ppm confirmed the presence of (-$OCH_3$). The $^{13}$C NMR (100 MHz, DMSO-$d_6$) showed the aldehyde carbon at $\delta$ 184.9 ppm, the methoxy carbon at $\delta$ 56.1 ppm, and other aromatic and heterocyclic carbons. The LC-MS spectrum showed a molecular ion peak at m/z 313.15 [M]$^{+}$, supporting the structure.

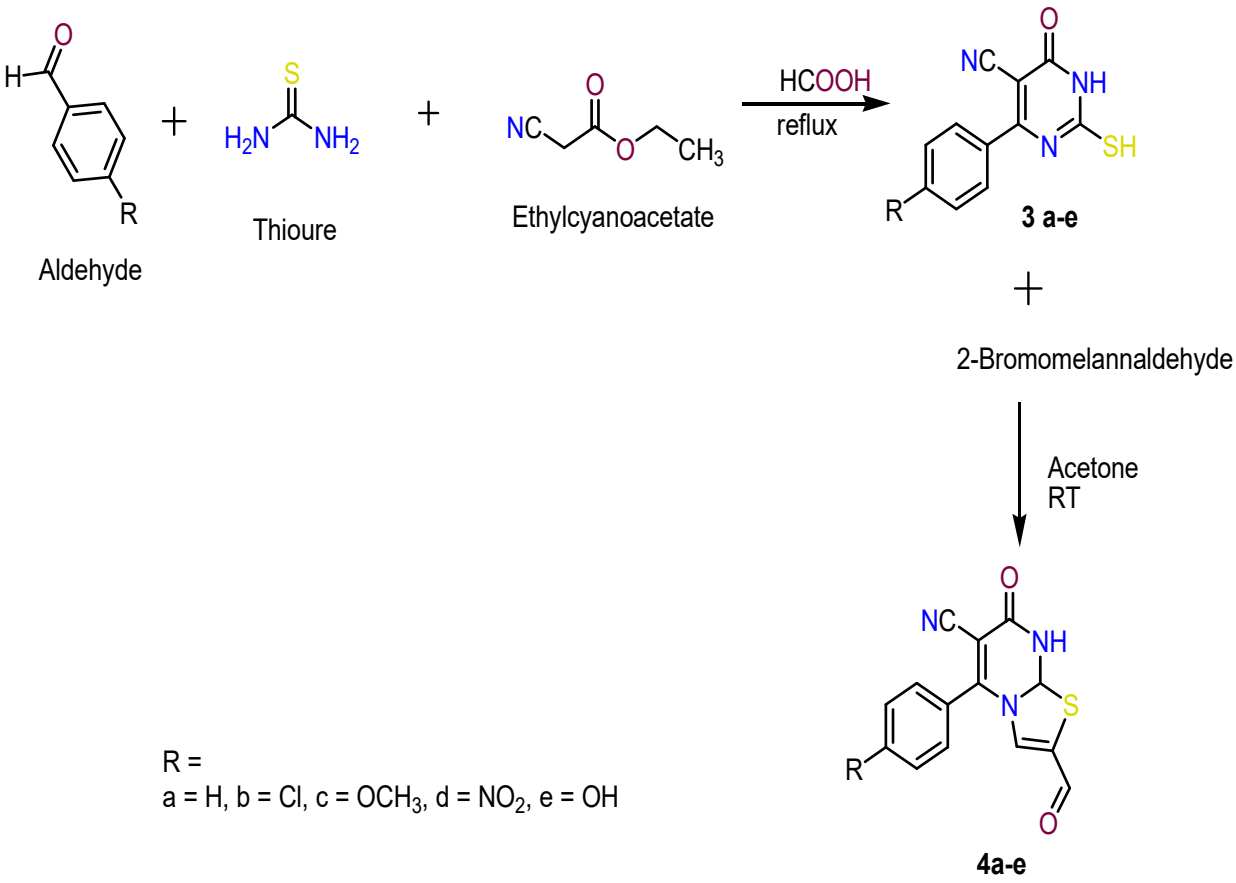


**Scheme 2**. Synthesis of thiazole pyrimidine-6-carbonitrile derivatives

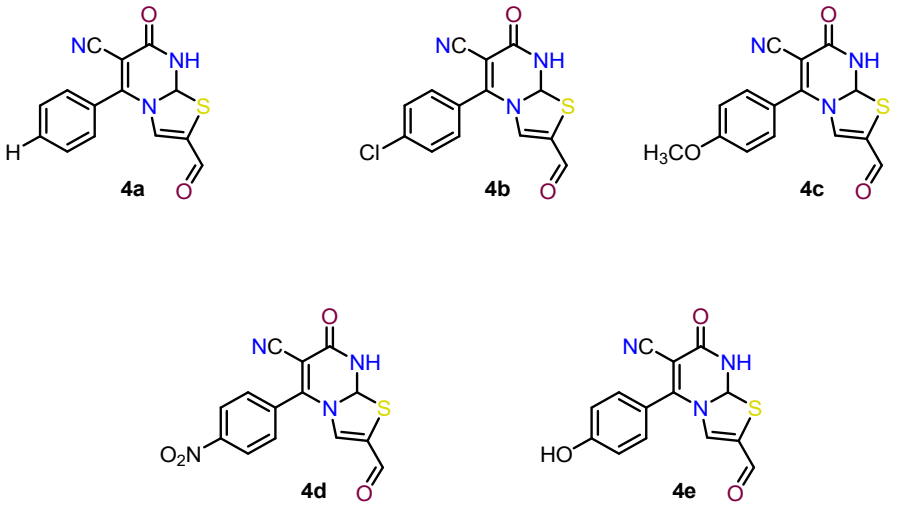


Synthesized thiazole pyrimidine-6-carbonitrile derivatives

### 2.2. Biological activity

#### 2.2.1. Antibacterial activity by macrodilution broth method

The synthesized compounds (**2a-d** and **4a-e)** were tested for their antibacterial activity against *Staphylococcus aureus*, *Streptococcus pyogenes*, *Salmonella typhi*, and *Pseudomonas aeruginosa* using the minimum inhibitory concentration (MIC) method. Streptomycin was used as the standard drug for comparison. Among all, compound **4a** showed

the best activity, with MIC values close to the standard drug (0.5-4 µg/mL). Compound **2b** also showed strong antibacterial activity with MICs between 1 and 4 µg/mL. On the other hand, compound **2c** was the least active, showing very high MIC values (128 to >512 µg/mL). Compounds **2a** and **4b** showed weak activity, while compounds **2d** and **4e** showed moderate activity with MIC values ranging from 2 to 8 µg/mL. Overall, compounds from the 4-series performed better than those from the 2-series, indicating that the changes made in their structure improved antibacterial activity. Compounds **4a** and **2b** may be considered as promising candidates for further development.

**Table 1.** Antibacterial activity of synthesized derivatives

| **Synthesized compounds** | **Minimum inhibitory concentration (µg/mL)** | | | |
|---|---|---|---|---|
| | ***S. aureus*** | ***S. pyogenes*** | ***S. typhi*** | ***P. aeruginosa*** |
| **2a** | 32 | 64 | 128 | 256 |
| **2b** | 1 | 1 | 4 | 4 |
| **2c** | 128 | 256 | 512 | >512 |
| **2d** | 8 | 8 | 32 | 32 |
| **4a** | 0.5 | 1 | 2 | 4 |
| **4b** | 128 | 256 | 256 | 512 |
| **4c** | 16 | 32 | 64 | 64 |
| **4d** | 8 | 16 | 32 | 32 |
| **4e** | 2 | 4 | 8 | 8 |
| **Strep** | 0.5 | 0.5 | 1 | 2 |

**2.2.2. Antioxidant activities: DPPH free radical scavenging activity**

The antioxidant potential of the synthesized compounds was evaluated using the DPPH free radical scavenging assay, and the results were expressed in terms of $IC_{50}$ values (µM). A lower $IC_{50}$ value indicates higher antioxidant activity. Among the tested compounds, **4a** ($IC_{50}$ = 36.43 µM) and **4e** ($IC_{50}$ = 37.37 µM) showed the highest activity, nearly equal to the standard compound **($IC_{50}$ = 37.37 µM).** Compound **2b** also exhibited good antioxidant activity with an $IC_{50}$ value of 38.72 µM. In contrast, compound **2c** was the least active **($IC_{50}$ = 66.33 µM).** These results suggest that compounds from the 4-series generally have better antioxidant potential than those from the 2-series.

The DPPH free radical scavenging potential (%) was calculated as follows:

$$\text{DPPH free radical scavenging potential (\%)} = [(\text{Ac} - \text{As})/\text{Ac}] \times 100$$

Where, Ac = absorbance of the control reaction mixture and As = absorbance of the test

**Table 2.** DPPH radical scavenging ability in terms of $IC_{50}$ values of synthetic compounds

| **Synthetic compounds** | **2a** | **2b** | **2c** | **2d** | **4a** | **4b** | **4c** | **4d** | **4e** | **Std** |
|---|---|---|---|---|---|---|---|---|---|---|
| **$IC_{50}$ (µM)** | 57.5 | 38.72 | 66.33 | 40.83 | 36.43 | 54.21 | 48.14 | 43.72 | 37.37 | 37.37 |

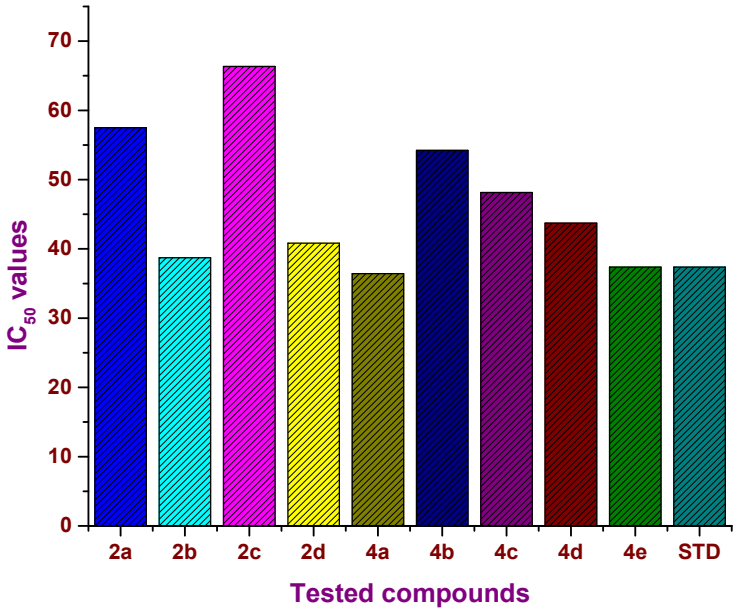


**Figure 3**. Graphical representations of the antioxidant activities

**2.2.3. Anti-inflammatory activity by % inhibition of protein denaturation**

The anti-inflammatory activity of the synthesized compounds was measured based on their ability to inhibit protein denaturation, and results were reported as $IC_{50}$ values (µM). A lower $IC_{50}$ value indicates stronger anti-inflammatory potential. Among all tested compounds, **4a** ($IC_{50}$ = 30.36 µM) and **4e** ($IC_{50}$ = 30.69 µM) showed the highest activity, closely followed by **2b** ($IC_{50}$ = 31.81 µM). Their activities were comparable to the standard drug **($IC_{50}$ = 31.03 µM).** On the other hand, compound **2c** showed the least activity with an $IC_{50}$ of 52.79 µM. Overall, compounds from the 4-series were more effective than those from the 2-series in reducing inflammation.

Percent inhibition of protein denaturation was determined using the following formula:

$$\text{Inhibition of protein denaturation (\%)} = [\frac{(\text{Ac} - \text{As})}{\text{Ac}}] \times 100$$

where Ac = absorbance of the control reaction mixture, As = absorbance of the test.

**Table 3.** Anti-inflammatory activity in terms of $IC_{50}$ values of the synthetic compounds

| **Synthetic compounds** | **2a** | **2b** | **2c** | **2d** | **4a** | **4b** | **4c** | **4d** | **4e** | **Std** |
|---|---|---|---|---|---|---|---|---|---|---|
| **$IC_{50}$ (µM)** | 46.75 | 31.81 | 52.79 | 33.76 | 30.36 | 41.37 | 39.50 | 36.79 | 30.69 | 31.03 |

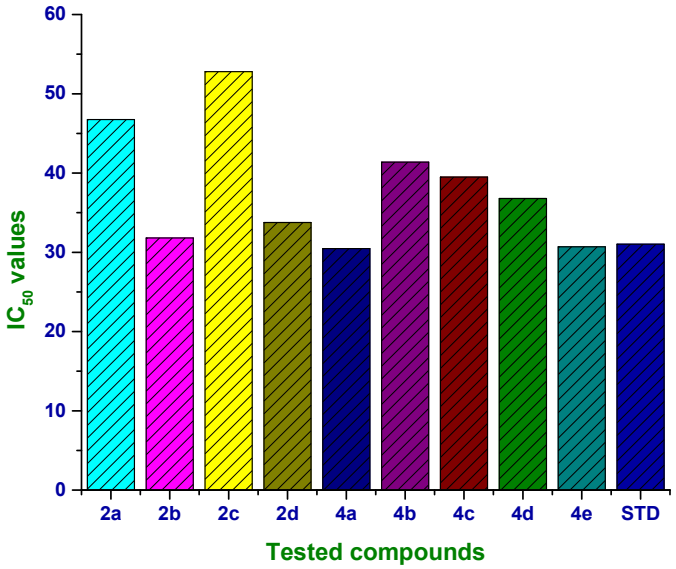


**Figure 4.** Graphical representations of the anti-inflammatory activities.

### 2.2.4. Inhibition of α-amylase activity

The synthesized compounds were evaluated for their antidiabetic activity by measuring the inhibition of α-amylase enzyme, expressed in terms of $IC_{50}$ values (μM). Lower $IC_{50}$ values indicate better enzyme inhibition. Among all, compound **4e** showed the strongest α-amylase inhibitory activity with an $IC_{50}$ of 39.62 μM, which was comparable to the standard ($IC_{50}$ = 40.83 μM). Other compounds such as **4b** ($IC_{50}$ = 42.06 μM) and **4c** ($IC_{50}$ = 43.81 μM) also displayed good activity. In contrast, compound **2b** exhibited the least activity ($IC_{50}$ = 70.24 μM). Overall, the 4-series compounds were more effective than the 2-series, suggesting improved α-amylase inhibition due to structural modifications.

Percent inhibition of α-amylase activity was determined using the following formula:

$$\text{Inhibition of } \alpha - \text{amylase activity } (\%) = \left[\frac{(Ac - As)}{Ac}\right] \times 100$$

where Ac = absorbance of the control reaction mixture, As = absorbance of the test.

**Table 4**. Inhibition of α-amylase activity of in terms of $IC_{50}$ values of the synthetic compounds

| Synthetic compounds | 2a | 2b | 2c | 2d | 4a | 4b | 4c | 4d | 4e | Std |
|---|---|---|---|---|---|---|---|---|---|---|
| $IC_{50}$ (μM) | 64.97 | 70.24 | 57.60 | 52.65 | 46.63 | 42.06 | 43.81 | 50.27 | 39.62 | 40.83 |

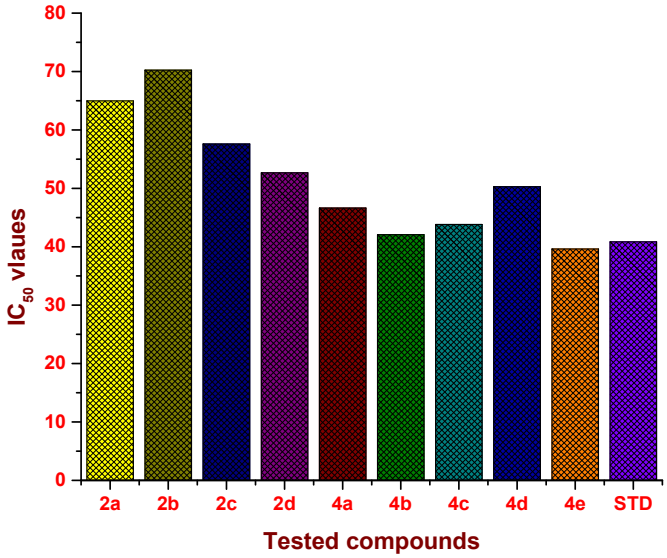


**Figure 5.** Graphical representations of the Inhibition of α-amylase activity.

**2.25 Inhibition of α-glucosidase activity**

The α-glucosidase inhibitory activity of the synthesized compounds was evaluated and expressed as $IC_{50}$ values (μM). A lower $IC_{50}$ value indicates stronger enzyme inhibition. Among all compounds, **4e** exhibited the highest inhibitory activity with an $IC_{50}$ of 29.94 μM, closely followed by **4b** (32.32 μM) and **4c** (33.51 μM). These values were comparable to the standard ($IC_{50}$ = 30.40 μM). In contrast, compound **2b** showed the weakest activity **($IC_{50}$ = 48.03 μM).** Overall, the 4-series compounds showed better α-glucosidase inhibition than the 2-series, highlighting the improved antidiabetic potential of the structurally modified derivatives. Percent inhibition of α-glucosidase activity was determined using the following formula:

$$Inhibition \text{ of } \alpha - \text{glucosidase activity } (\%) = [\frac{(Ac - As)}{Ac}] \times 100$$

where Ac = absorbance of the control reaction mixture, As = absorbance of the test.

**Table 5.** Inhibition of α-glucosidase activity of in terms of $IC_{50}$ values of the synthetic compounds

| Synthetic compounds | 2a | 2b | 2c | 2d | 4a | 4b | 4c | 4d | 4e | Std |
|---|---|---|---|---|---|---|---|---|---|---|
| $IC_{50}$ (μM) | 44.23 | 48.03 | 42.34 | 38.88 | 36.43 | 32.32 | 33.51 | 37.90 | 29.94 | 30.40 |

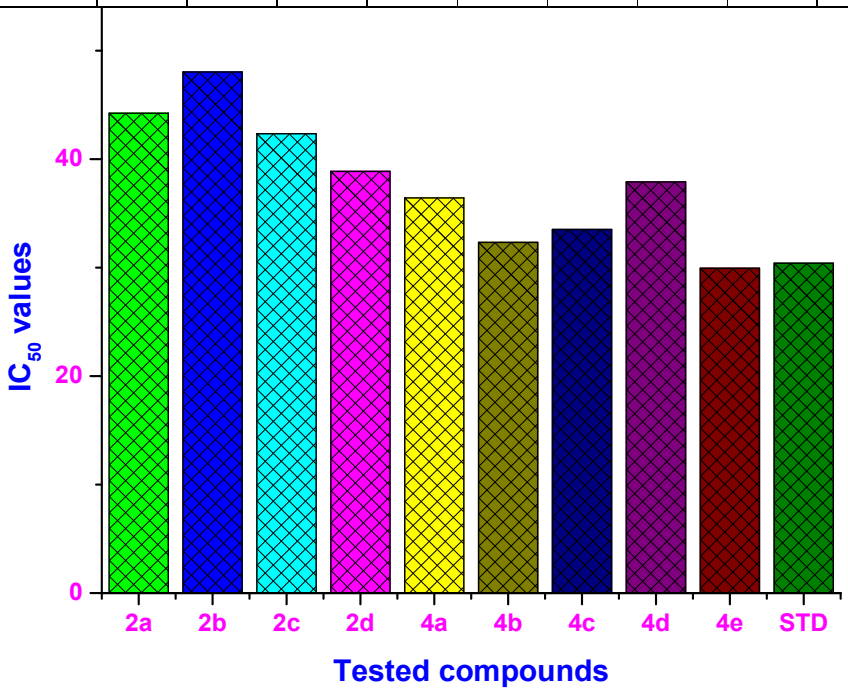


**Figure 6.** Graphical representations of the Inhibition of α-glucosidase activity

**2.2.5. Anticancer studies**

Based on antioxidant and anti-inflammatory studies, we have chosen compounds **2b** and **4a** for the anticancer studies.

**Table 6:** $IC_{50}$ values of the selected compounds on U87MG, MCF7 and A549 cells

| Compounds/Cells | U87MG | MCF7 | A549 |
|---|---|---|---|
| | $IC_{50}$ (μg/mL) | | |
| **2b** | 55.81 | 50.5 | 45.01 |
| **4a** | 52.41 | 34.38 | 39.82 |

Compounds **2b** and **4a** were tested for their cytotoxic effects on three human cancer cell lines: A549 (lung carcinoma), MCF7 (breast cancer), and U87MG (glioblastoma). **Table 6** provides a summary of the $IC_{50}$ values. The inhibitory effects of both drugs were moderate, although **4a** was more potent than **2b** across all evaluated cell lines.

Comparing compound **2b** to U87MG, the $IC_{50}$ values were 55.81 µg/mL, 50.5 µg/mL, and 45.01 µg/mL, respectively. Comparatively, compound **4a** showed increased cytotoxic activity with lower $IC_{50}$ values of 52.41 µg/mL in U87MG, 34.38 µg/mL in MCF7, and 39.82 µg/mL in A549 cells. Compound **4a** showed the highest cytotoxicity against MCF7 cells ($IC_{50}$ = 34.38 µg/mL).

The consistently lower $IC_{50}$ values of compound **4a** showed that it was more effective than compound **2b** overall across all three cell lines. This implies that the structural modifications made in **4a** might help improve interaction with cellular targets essential for the survival and growth of cancer cells. This compound exhibited the maximum sensitivity in MCF7 breast cancer cells, with an $IC_{50}$ of 34.38 µg/mL, which was significantly lower than that of compound **2b** (50.5 µg/mL). This suggests that **4a** may have a preferential cell-killing effect on breast cancer cells, which could be linked to signalling pathways for hormone receptors or altered cellular drug uptake processes in these cells. In A549 lung cancer cells, both compounds exhibited moderate cytotoxic activity; however, **4a** was once more superior (39.82 µg/mL vs. 45.01 µg/mL).

According to the findings, unsubstituted phenyl increases its cytotoxic activity, possibly by enhancing its lipophilicity, cellular permeability, or binding affinity to certain molecular targets. Although higher concentrations were required than for MCF7 and A549. The moderate efficacy against glioblastoma (U87MG) further demonstrates **4a**'s ability to possess cytotoxic effects even on highly resistant cancer types.

### 2.2.6. Apoptosis detection by dual fluorescence staining

This assay is based on the principle of differential staining, wherein acridine orange stains the nuclei of viable as well as apoptotic cells, while ethidium bromide selectively stains the nuclei of the cells undergoing apoptosis. The green channel represents the nuclei stained with acridine orange, and the red channel represents the nuclei stained with ethidium bromide. Greenish-yellow nuclei under the merge channel represent the early apoptotic cells.

In our study, the compounds **2b** and **4a** induced early apoptosis in all three cancer cell types studied, namely A549, MCF7, and U87MG, as visualized by the appearance of greenish-yellow nuclei under the merge channel. Fluorescence micrographs of the cells are represented in Figures **6, 7,** and **8**.

When compared to untreated controls, a clear change in nuclear morphology was observed under a fluorescent microscope after treatment. The control group's viable cells had consistently green nuclei, which suggested that the chromatin was intact. On the other hand, thiazolopyrimidine-treated nuclei fluoresced greenish-yellow, indicating chromatin condensation and fragmentation, two hallmarks of early apoptosis.

The proportion of cells exhibiting apoptotic characteristics differed between the cell lines. While U87MG cells showed significantly fewer modifications, MCF7 and A549 cells showed a comparatively larger population of early apoptotic nuclei, which is in agreement with the resistance nature of glioblastoma cells to chemotherapeutic agents. It was further seen that the synthetic compounds mostly induced early apoptotic events rather than late apoptosis or necrosis by the visualization of greenish-yellow nuclei over orange/red nuclei.

According to these results, thiazolopyrimidines may exert cytotoxicity via triggering signaling pathways leading to programmed cell death. Because these synthetic analogs cause early apoptosis, it is possible that they interact with intracellular targets regulating caspase activation or mitochondrial integrity. Their potential as promising anticancer leads against lung, breast, and brain malignancies is highlighted by the selective apoptosis induction observed in MCF7, A549, and U87MG cells.

Thiazolopyrimidines are reported to possess cytotoxic activity on cancer cells. Two new sets of thiazolopyrimidines synthesized were reported to exert potential anticancer activity against both MCF-7 breast cancer and HepG2 liver cancer cells, with $IC_{50}$ ranges of (24.52-30.22 and 21.49-34.09 µM), respectively, via the inhibition of cell proliferation and apoptosis[27]. The MTT assay was employed to assess the antitumor activity of the thiazolopyrimidines *in vitro* against hepatocellular carcinoma (HepG-2), human prostate cancer (PC-3), and human colorectal cancer cells (HCT-116). All the studied derivatives demonstrated dose-dependent anticancer activity in three different types of cancer cells[28]. Our results are further supported by the inference reported in these investigations.

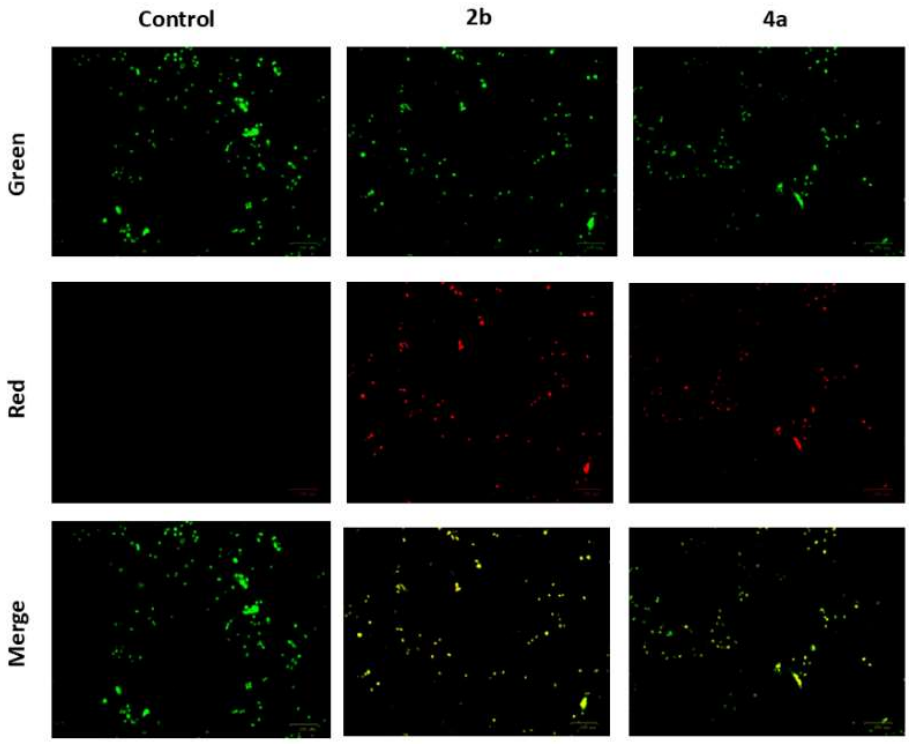


**Figure 7.** Photomicrographs of A549 control and treated cells. Magnification 20X

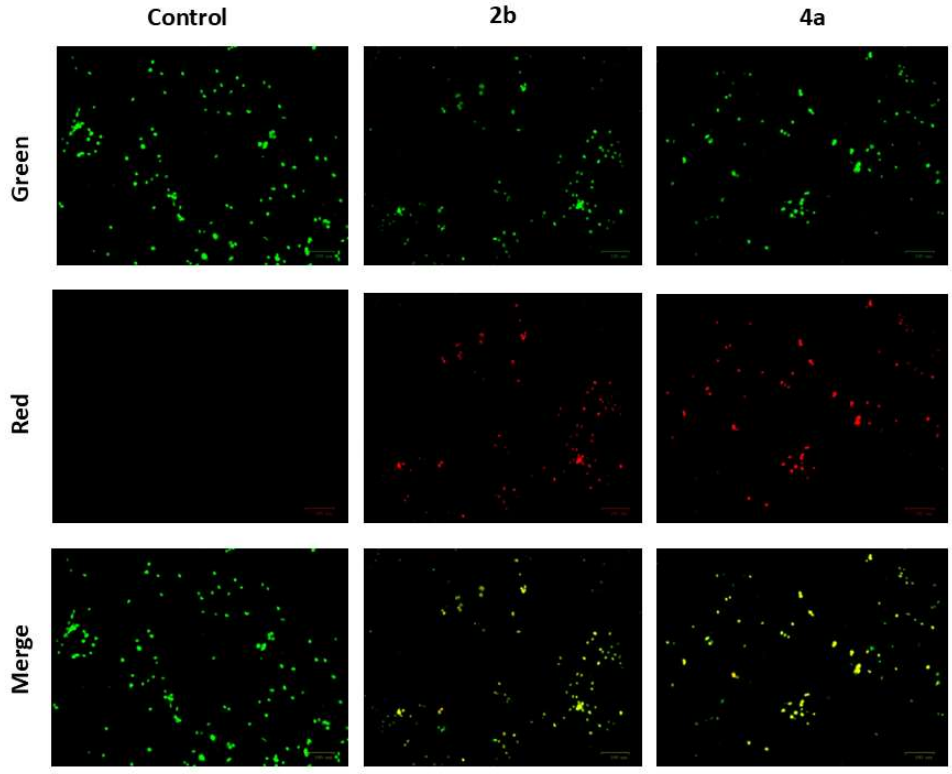


**Figure 8.** Photomicrographs of MCF7 control and treated cells. Magnification 20X

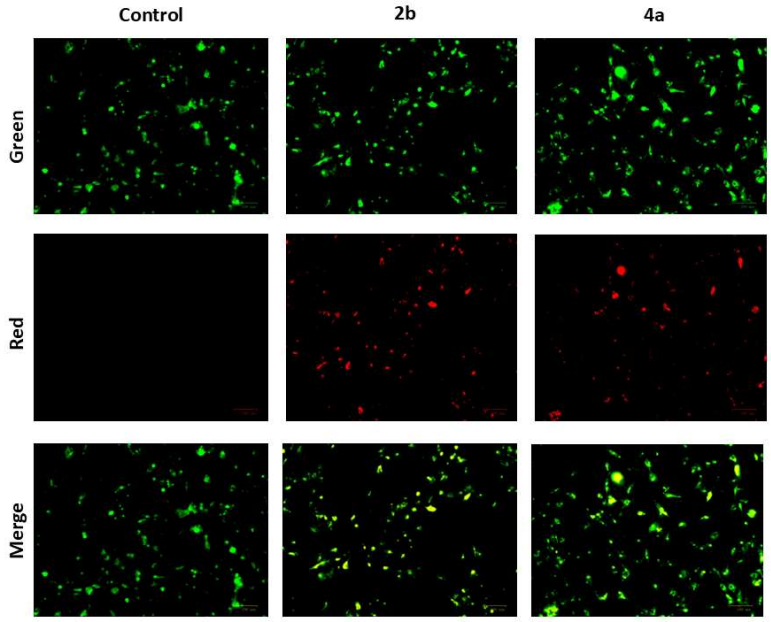


**Figure 9.** Photomicrographs of U87MG control and treated cells. Magnification 20X

### 2.2.7. Molecular docking studies

Molecular docking analysis was carried out to estimate the binding affinities of the most active compounds, **2b** and **4a,** against key protein targets involved in cancer. The docking results revealed that compound 4a exhibited stronger binding affinities compared to **2b** across all three targets. Against the EGFR kinase domain (PDB ID: 1XKK) relevant to A549 lung cancer cells, compound **4a** showed a binding affinity of –8.4 kcal/mol, better than **2b** (–7.4 kcal/mol). For BRD2 (PDB ID: 6JKE), related to U87MG glioblastoma cells, **4a** showed –7.9 kcal/mol, while **2b** showed –6.6 kcal/mol. With the Estrogen Receptor alpha (PDB ID: 3ERT) for MCF-7 breast cancer cells, **4a** also showed higher affinity (–8.2 kcal/mol) than **2b** (–6.9 kcal/mol). These results support the experimental data, indicating that compound **4a** has a stronger and more stable interaction with cancer-related targets, suggesting its promising potential as an anticancer agent.

**Table 7:** Molecular Docking Results of Compounds **2b** and **4a** Against Cancer-Associated Targets

| **Activity** | **PDB** | **Binding Affinity (kcal/mol)** | |
|---|---|---|---|
| | | **2b** | **4a** |
| **A549** | EGFR kinase domain complexed with a quinazoline inhibitor-GW572016 (1XKK) | -7.4 | -8.4 |
| **U87MG** | Crystal structure of NS5 in complex with the N-terminal bromodomain of BRD2. (6JKE) | -6.6 | -7.9 |
| **MCF 7** | Human Estrogen Receptor Alpha Ligand-Binding Domain in complex with 4-Hydroxytamoxifen (3ERT) | -6.9 | -8.2 |

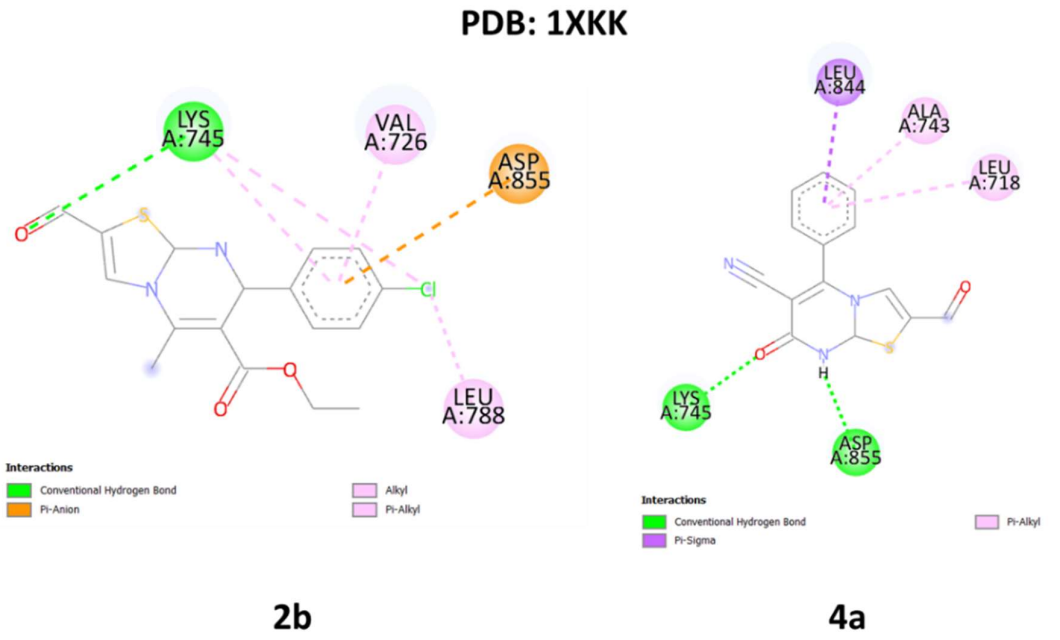


**Figure 10.** 2D Interaction Diagrams of Compounds **2b** and **4a** with EGFR Kinase Domain (PDB: 1XKK)

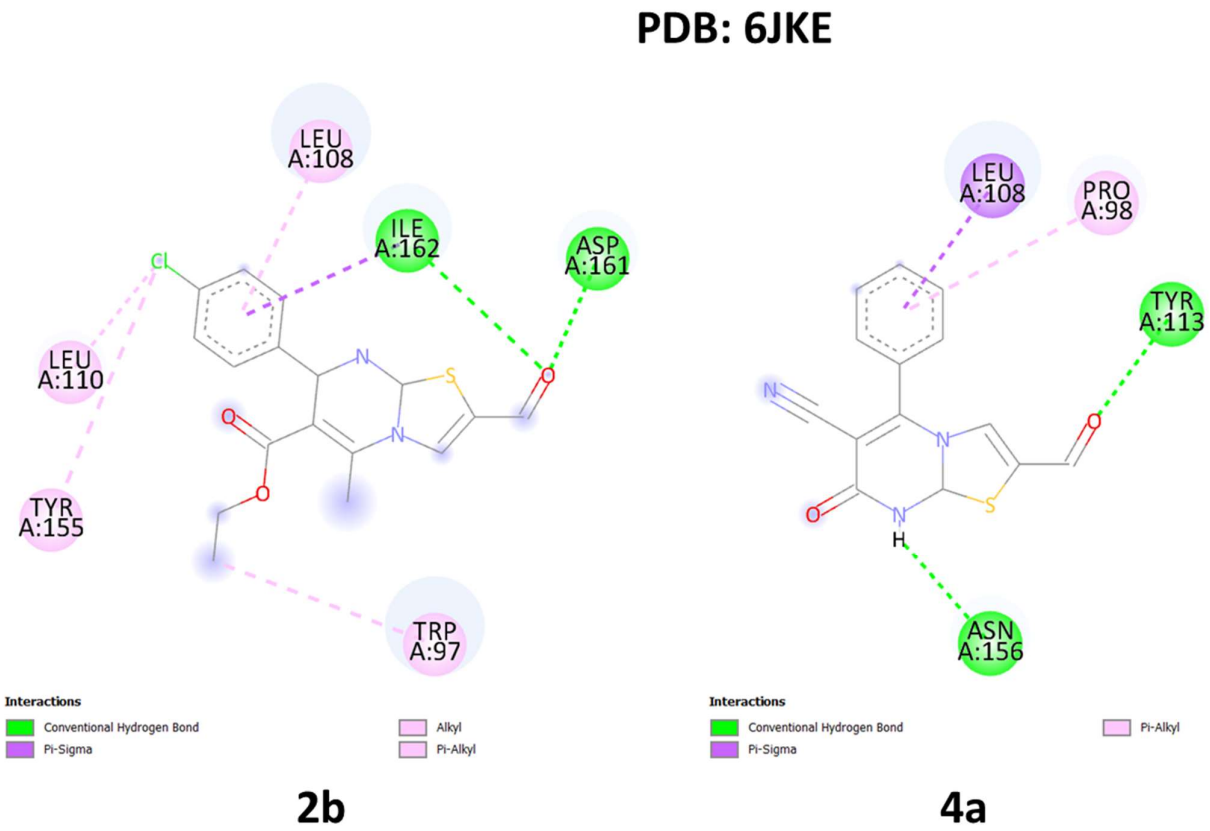


**Figure 11.** 2D Interaction Diagrams of Compounds **2b** and **4a** with BRD2 Bromodomain (PDB: 6JKE)

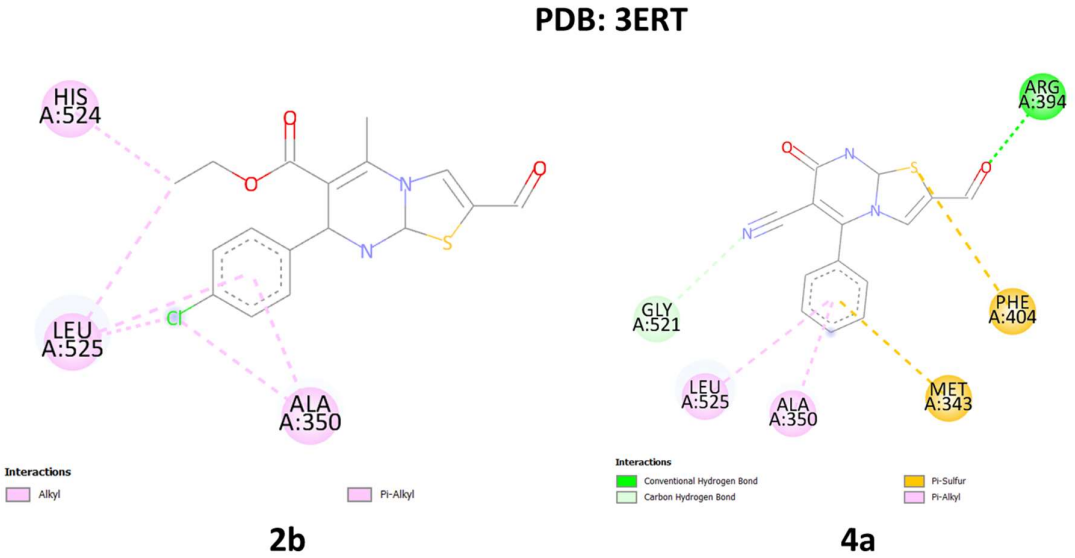


**Figure 12.** 2D Interaction Diagrams of Compounds **2b** and **4a** with Estrogen Receptor Alpha (PDB: 3ERT)

## 3. EXPERIMENTAL

### 3.1 Chemistry

#### 3.1.1 General

The melting points of the prepared compounds were detected by the open capillary method. Infrared spectra were acquired using an FTIR spectrophotometer by the ATR technique. A JEOL 400 MHz NMR spectrometer was used to record $^1$H NMR spectra with DMSO-*d*6 as the solvent and TMS as the internal standard. Proton signals were identified as singlet (s), doublet (d), triplet (t), and multiplet (m). All values are reported using the $\delta$ scale with respect to TMS, and mass spectra were generated using a Micro Mass Quattro Micro API mass spectrometer.

#### 3.1.2. Synthesis of ethyl 2-formyl-5-methyl-7-phenyl-8,8*a*-dihydro-7*H*-thiazolo[3,2-*a*]pyrimidine-6-carboxylate (2a-d)

A mixture of thiourea (1.5 mmol), aldehyde derivatives (1.0 mmol), and ethyl acetoacetate was heated at 70 °C for the required time in the presence of formic acid (10 mL) to promote the condensation and cyclization of the reactants during the synthesis. After the reaction completion, the reaction mixture was cooled, followed by the addition of cold water, resulting solid was filtered and purified through recrystallization from ethanol to obtain the pure product (**1a-d**).[29] Then the mixture of the synthesized product (**1a-d**) and 2-bromo-malonaldehyde was stirred in acetone as a solvent at room temperature for about 16 hours, the extra solvent was added with ice cubes, and neutralized with sodium bicarbonate, and the solid product was isolated by filtration and recrystallized from ethanol to get the pure product (**2a-d**).

**Ethyl2-formyl-5-methyl-7-phenyl-8,8*a*-dihydro-7*H*-thiazolo[3,2-*a*]pyrimidine-6-carboxylate (2a)**

Yield: 85%; Yellow coloured solid; Melting point: 182-184 °C; FTIR (cm$^{-1}$): 3042 (N-H), 1701 (C=O), 1308 (C-S), 1238 (C-N), 764 (C-H); $^1$H NMR (DMSO, 400 MHz): $\delta$ 9.62 (s, CHO, 1H), 8.46 (s, N-H, 1H), 7.37 (t, $J$ = 4.0 and 8.0 Hz, Ar-H, 5H), 6.93 (s, Th-H, 1H), 6.38 (s, Ar-H, 1H), 5.67 (s, Ar-H, 1H), 3.42 (m, $J$ = 4.0 and 8.0 Hz, Ar-H, 2H), 2.34 (s, $CH_3$, 3H), 1.07 (t, $J$ = 8.0 Hz, ester-$CH_3$, 3H); $^{13}$C NMR (DMSO, 100 MHz): $\delta$ 182.6, 165.7, 162.8, 154.2, 144.1, 142.8, 140.4, 139.2, 129.5, 129.2, 129.0, 128.0, 127.6, 127.2, 122.0, 117.91, 102.7, 60.0, 59.2, 23.5, 14.4, 14.2; LCMS: 330.10[M+]; Elemental analysis of $C_{17}H_{18}N_2O_3S$: Calculated: C (61.80 %), H (5.49 %), N (8.48 %); Found: C (61.10 %), H (5.21 %), N (8.02 %).

**Ethyl 7-(4-chlorophenyl)-2-formyl-5-methyl-8,8*a*-dihydro-7*H*-thiazolo[3,2-*a*]pyrimidine-6-carboxylate (2b)**

Yield: 82%; Yellow coloured solid; Melting point: 144-146 °C; FTIR (cm$^{-1}$): 3031 (N-H), 1704 (C=O), 1370 (C-S), 1235 (C-N), 717 (C-H); $^1$H NMR (DMSO, 400 MHz): $\delta$ 9.62 (s, CHO, 1H), 8.33 (s, N-H, 1H), 7.43 (m, $J$ = 8 Hz, Ar-H, 5H), 6.69 (s, Th-H, 1H), 6.42 (s, Ar-H, 1H), 4.00 (m, $J$ = 8 Hz, $CH_2$, 2H), 2.35 (s, $CH_3$, 3H), 1.09 (t, $J$ = 8 Hz, ester-$CH_3$, 3H); $^{13}$C NMR (DMSO, 100 MHz): $\delta$ 182.6, 165.6, 162.8, 141.7, 141.6, 133.9, 131.6, 129.8, 129.5, 129.0, 128.8, 128.6, 122.2, 102.3, 60.1, 58.5, 23.5, 14.4; LCMS: 364.10 [M+], 366.24 [M+2]; Elemental analysis of $C_{17}H_{17}N_2ClO_3S$: Calculated: C (55.96 %), H (4.70 %), N (7.68%); Found: C (55.63 %), H (4.02 %), N (7.38 %).

**Ethyl 2-formyl-7-(4-methoxyphenyl)-5-methyl-8,8*a*-dihydro-7*H*-thiazolo[3,2-*a*]pyri midi ne-6-carboxylate (2c)**

Yield: 87%; Yellow coloured solid; Melting point: 200-202 °C; FTIR (cm$^{-1}$): 2990 (C-H), 1698 (C-N), 1507 (C=C), 1027 (C=S), 791 (C-H); $^1$H NMR (DMSO, 400 MHz): $\delta$ 9.61 (s, CHO, 1H), 8.32 (s, N-H, 1H), 7.29 (d, $J$ = 8.0 Hz, Ar-H, 2H), 6.93 (d, $J$ = 8.0 Hz, Ar-H, 2H), 6.32 (s, Th-H, 1H), 4.0 (m, $J$ =

4.0 and 8.0 Hz, $CH_2$, 2H), 3.73 (s, $OCH_3$, 3H), 3.37 (s, Ar-H, 1H) 2.34 (s, $CH_3$, 3H), 1.09 (t, *J* = 8.0 Hz, ester-$CH_3$, 3H); $^{13}$C NMR (DMSO, 100 MHz): *δ* 182.5, 165.8, 165.5, 162.5, 159.9, 153.8, 141.9, 135.1, 128.6, 121.9, 114.7, 114.3, 102.9, 60.0, 58.7, 55.6, 23.4, 14.4; LCMS: 359.23[M+]; Elemental analysis of $C_{18}H_{20}N_2O_4S$ :Calculated: C (59.98%), H (5.59%), N (7.77%); Found: C (59.75%), H (5.19%), N (7.27%).

**Ethyl 2-formyl-7-(4-hydroxyphenyl)-5-methyl-8,8*a*-dihydro-7*H*-thiazolo[3,2-*a*] pyramid ine-6-carboxylate (2d)**

Yield: 84%; Yellow coloured solid; Melting point: 160-162 °C; FTIR (cm$^{-1}$): 3172 (N-H), 1708 (C=O), 1592 (C=N), 1507 (C-H), 1223 (C=S), 791 (C-H), 720 (C-S); $^1$H NMR (DMSO, 400 MHz): *δ* 9.79 (s, CHO, 1H), 8.63 (s, N-H, 1H), 7.30 (d, *J* = 8.0 Hz, Ar-H, 2H), 6.78 (d, *J* = 8.0 Hz, Ar-H, 2H), 6.51 (s, Th-H, 1H), 6.19 (s, Ar-H, 1H), 4.03 (t, *J* = 4.0 and 8.0 Hz, OH and $CH_2$ , 3H), 2.45 (t, *J* = 28.0 Hz, $CH_3$, 3H), 1.08 (t, *J* = 4.0 and 8.0 Hz, ester-$CH_3$, 3H); $^{13}$C NMR (DMSO, 100 MHz): *δ* 183.1, 164.6, 161.5, 158.8, 140.4, 131.3, 129.5, 116.2, 103.9, 60.8, 60.2, 31.2, 19.6, 14.4; LCMS: 346.18[M+]; Elemental analysis of $C_{17}H_{18}N_2O_4S$: Calculated: C (58.94%), H (5.24 %), N (8.09 %); Found: C (58.02%), H (5.01%), N (7.99%).

**3.1.3. Synthesis of 2-Formyl-7-oxo-5-phenyl-8,8*a*-dihydro-7*H*-thiazolo[3,2-*a*]pyrimidine-6-carbonitrile (4a-e)**

A mixture containing the corresponding benzaldehyde (0.01 mol), ethyl cyanoacetate (0.01 mol), sodium carbonate (0.01 mol), and thiourea (0.01 mol) in ethanol (30 mL) was refluxed for 6 h. After cooling, the resulting product was collected by filtration, washed, and dried. The solid was then dissolved in water (20 mL) and heated at 80-90 °C until it turned to a clear solution. Upon cooling, acidified the solution with acetic acid and stirred for 30 min. The separated solid was filtered, washed with cold water, dried, and recrystallized from ethanol to get the pure compounds (**3a-e**).[30]

Then the mixture of the synthesized product and 2-bromomalonaldehyde was stirred in acetone as a solvent. The reaction was kept at RT for approximately 16 hours, after which the excess solvent was removed. Added ice cubes and neutralized with sodium bicarbonate, and the solid was separated by filtration and recrystallized from ethanol to obtain the pure products (**4a-e**).

**2-Formyl-7-oxo-5-phenyl-8,8*a*-dihydro-7*H*-thiazolo[3,2-*a*]pyrimidine-6-carbonitrile (4a)**

Yield: 88%; Yellow-colored solid; Melting point: 186-188 °C; FTIR (cm$^{-1}$): 3103 (N-H), 2225 (C-H), 1680 (C=O), 1578 (C=N), 1498 (C=S), 780 (C-S); $^1$H NMR (DMSO, 400 MHz): *δ* 10.05 (s, CHO, 1H), 8.7 (s, N-H, 1H), 8.07 (t, *J* = 8.0 Hz, Ar-H, 2H), 7.62 (d, *J* = 8.0 Hz, Ar-H, 2H), 7.58 (d, *J* = 8.0 Hz, Ar-H, 2H), 7.53 (d, *J* = 8.0 Hz, Ar-H, 2H), 7.26 (s, Ar-H, 1H), 5.40 (s, Th-H, 1H); $^{13}$C NMR (DMSO, 100 MHz): *δ* 180.8, 168.4, 164.2, 156.7, 134.6, 132.7, 130.7, 129.8, 129.3, 129.0, 128.9, 114.6, 90.8; LCMS: 284.34[M+]: Elemental analysis of $C_{14}H_9N_3O_2S$: Calculated: C (59.35%), H (3.20 %), N (14.83 %); Found: C (58.99 %), H (3.01%), N (14.23 %).

**5-(4-Chlorophenyl)-2-formyl-7-oxo-8,8*a*-dihydro-7*H*-thiazolo[3,2-*a*]pyrimidine-6-carbonitrile (4b)**

Yield: 83%; Yellow-colored solid; Melting point: 166-168 °C; FTIR (cm$^{-1}$): 3572 (N-H), 2965 (C-H), 1636 (C=N), 1468 (C=C), 766 (C-S); $^1$H NMR (DMSO, 400 MHz): *δ* 10.06 (s, CHO, 1H), 9.30 (s, N-H, 1H), 8.06 (t, *J* = 4.0 and 8.0 Hz, Ar-H ,1H), 8.01 (d, *J* = 4.0 Hz, Ar-H ,1H), 7.61 (t, *J* = 4.0 and 12.0 Hz, Ar-H, 2H), 7.54 (t, *J* = 8.0 Hz, Ar-H, 1H), 7.39 (S, $CH_3$, 3H), 5.40 (s, Th-H, 1H); $^{13}$C NMR (DMSO, 100 MHz): *δ* 184.8, 166.9, 166.4, 165.9, 163.5, 157.4, 137.4, 135.5, 134.2, 131.8, 130.1, 128.9, 117.4, 115.9, 90.4, 70.8, 62.7, 59.0, 34.0, 14.2; LCMS: 317.43 [M+], 319.21 [M+2]; Elemental analysis of $C_{14}H_8N_3ClO_2S$: Calculated: C (52.92 %), H (2.54 %), N (13.22 %); Found: C (52.73%), H (1.99 %), N (12.99 %).

**2-Formyl-5-(4-methoxyphenyl)-7-oxo-8,8*a*-dihydro-7*H*-thiazolo[3,2-*a*]pyrimidine-6-carbonitrile (4c)**

Yield: 81%; Yellow-colored solid; Melting point: 172-174 °C; FTIR (cm$^{-1}$): 3085 (N-H), 2215 (C-H), 1665 (C=N), 1571 (C=C), 692 (C-S); $^1$H NMR (DMSO, 400 MHz): *δ* 10.09 (s, CHO, 1H), 9.24 (s, N-H, 1H), 8.03 (d, *J* = 8.0 Hz, Ar-H, 2H), 7.15 (d, *J* = 12.0 Hz, Ar-H, 3H), 5.56 (s, Th-H, 1H), 3.87 (S, $OCH_3$, 3H); $^{13}$C NMR (DMSO, 100 MHz): *δ* 184.9, 163.0, 155.2, 147.3, 143.8, 143.7, 134.5, 130.4, 122.9, 116.9, 116.8, 107.8, 107.4, 62.2; LCMS: 313.15[M+]; Elemental analysis of $C_{15}H_{11}N_3O_3S$: Calculated: C (57.50 %), H (3.54 %), N (13.41 %); Found: C (57.30 %), H (3.24 %), N (7.01 %).

**2-Formyl-5-(4-nitrophenyl)-7-oxo-8,8*a*-dihydro-7*H*-thiazolo[3,2-*a*]pyrimidine-6-carb onitrile (4d)**

Yield: 79%; Yellow colored solid; Melting point: 177-179 °C; FTIR (cm$^{-1}$): 3287 (N-H), 2227 (C-H), 1587 (C=N), 1518 (C=C), 1012 (C=S), 634 (C-S); $^1$H NMR (DMSO, 400 MHz): *δ* 10.12 (s, CHO, 1H), 9.34 (s, N-H, 1H), 8.43 (t, *J* = 8.0 Hz, Ar-H, 2H), 8.18 (m, *J* = 4.0 Hz, Ar-H, 2H), 7.31 (s, Ar-H, 1H), 5.54 (s, Th-H, 1H); $^{13}$C NMR (DMSO, 100 MHz): *δ* 163.4, 163.0, 134.5, 123.0, 117.0, 116.9, 97.5, 62.4, 14.5; LCMS: 328.13[M+]; Elemental anslysis of $C_{14}H_8N_4O_4S$: Calculated: C (51.22 %), H (2.46 %), N ( 17.07 %); Found: C (50.99 %), H (2.22 %), N (16.97 %).

**2-Formyl-5-(4-hydroxyphenyl)-7-oxo-8,8*a*-dihydro-7*H*-thiazolo[3,2-*a*]pyrimidine-6-carbonitrile (4e)**

Yield: 80%; Yellow-colored solid; Melting point: 178-180 °C; FTIR (cm$^{-1}$): 3354 (N-H), 1576 (C=N), 1442 (C-H), 700 (C-S); $^1$H NMR (DMSO, 400 MHz): *δ* 9.99 (s, CHO, 1H), 9.22 (s, N-H, 1H), 8.24

(s, Ar-H, 1H), 8.00 (d, *J* = 4.0 Hz, Ar-H, 2H), 6.95 (d, *J* = 8.0 Hz, Ar-H, 2H), 5.49 (s, Th-H, 1H), 4.44 (s, O-H, 1H); $^{13}$C NMR (DMSO, 100 MHz): $\delta$ 184.9, 163.4, 163.1, 155.2, 134.5, 130.4, 123.0, 116.9, 116.8, 107.9, 107.3, 62.4; LCMS: 328.13[M+]; Elemental analysis of $C_{14}H_9N_3O_3S$: Calculated: C (56.18 %), H (3.03 %), N (14.04%); Found: C(55.92%), H (2.01%), N (14.02%).

**3.2. Biological assay**

**3.2.1. Antibacterial activity by the macrodilution broth method:**

The synthesized compounds were tested for their antibacterial efficiency by the macrodilution broth method as per CLSI guidelines.[31] The antibacterial studies of the compounds were evaluated by determining their minimum inhibitory concentration (MIC). The test organisms included two Gram-positive bacteria, *Streptococcus pyogenes* (ATCC® 19615™), *Staphylococcus aureus* subsp. *aureus* (ATCC® 6538P™) and two Gram-negative bacteria, *Pseudomonas aeruginosa* (ATCC® 27853™) and *Salmonella enterica* subsp. *enterica* serovar Typhimurium (ATCC® 14028™). Briefly, 18 h old cultures of test bacterial pathogens were subjected to dilution following a 0.5 McFarland turbidity standard to obtain a bacterial load of $5\times 10^5$ CFU/mL in each test tube containing 2 mL sterile Mueller-Hinton broth. Compounds at different concentrations (0.25, 0.5, 1, 2, 4, 8, 16, 32, 64, 128, 256, and 512 µg/mL) were put in test tubes that had been infected and correspondingly labelled. After thoroughly mixing, the tubes were incubated for 24 hours at 37 °C. MIC values are the lowest concentrations of chemicals that prevent bacteria from growing visibly. Streptomycin was a common antibacterial medication.

**3.2.2. Antioxidant activities: DPPH free radical scavenging activity**

The antioxidant studies of the synthesized compounds were assessed using the free radical scavenging assay DPPH, according to the procedure reported by Brand-Williams et al [32]. Two mL of DPPH solution (0.1 mM in methanol) were combined with one mL of the produced compounds at various concentrations (20, 40, 60, 80, and 100 µg/mL). After mixing the tubes, they were left at room temperature for 30 minutes in the dark. The antioxidant activity was assessed using ascorbic acid as the standard antioxidant agent and 1 mL of solvent (50% DMSO) in 2 mL of DPPH solution as a control. At 517 nm, the absorbance was measured. The free DPPH radical scavenging potential (%) was calculated as follows:

$$\text{DPPH free radical scavenging potential (\%)} = [(\text{Ac} - \text{As})/\text{Ac}] \times 100$$

Where Ac = absorbance of the control reaction mixture and As = absorbance of the test

**3.2.3. Anti-inflammatory activity by % inhibition of protein denaturation**

The anti-inflammatory activity of synthesized compounds was determined by % inhibition of protein denaturation assay as described by Altundag *et al.* [33] One mL of 0.1% bovine serum albumin, 3 mL of PBS (pH 6.4), and one mL of different quantities (20, 40, 60, 80, and 100 µg/mL) of produced compounds were combined and carefully mixed. After 20 minutes of incubation at 37 °C, the tubes were heated for an additional five minutes at 70 °C. After adding 1 mL of 1% Folin-Ciocalteu's reagent and one mL of alkaline copper reagent to 1 mL of the reaction mixture, the mixture was incubated at 55 °C for 10 minutes. The absorbance at 650 nm was then tested. 50% DMSO served as the control, and diclofenac sodium served as the standard

Percent inhibition of protein denaturation was determined using the following formula:

$$\text{Inhibition of protein denaturation (\%)} = [\frac{(\text{Ac} - \text{As})}{\text{Ac}}] \times 100$$

where Ac = absorbance of the control reaction mixture, As = absorbance of the test.

**3.2.4. Inhibition of α-amylase activity**

The antidiabetic activity, expressed as the % inhibition of α-amylase, was determined by taking the 3,5-dinitrosalicylic acid (DNS) method.[34] Shortly, 100 µL of 1% α-amylase solution was mixed with 100 µL of the test compounds at varying concentrations (20, 40, 60, 80, and 100 µg/mL) and pre-incubated for 30 minutes. α-amylase and pure water were used as a control. After adding 100 µL of 1% starch, the mixture was incubated at 37 °C for 10 minutes, after which 200 µL of 3,5-dinitrosalicylic acid (DNSA) reagent was added to each test. After that, for five minutes incubated the test tubes in a hot water bath. Once the tubes were cooled, the OD was measured at 540 nm. Acarbose was a common medication.

Percent inhibition of α-amylase activity was determined using the following formula:

$$Inhibition(\%) = [\frac{(Ac - At)}{Ac}] \times 100$$

where Ac = absorbance of the control reaction mixture, At = absorbance of the test

**3.2.5. Inhibition of α-glucosidase activity**

The antidiabetic activity of the synthesized compounds was further evaluated through their ability to inhibit α-glucosidase activity[35] Briefly, varying concentrations of the test compounds (20, 40, 60, 80, and 100 µg/mL) were pre-incubated with 200 µL of 1% α-glucosidase and 500 µL of PBS buffer (100 mM, pH 7.2) at 37 °C for 30 minutes. Subsequently, 400 µL of p-nitrophenyl-α-D-glucopyranoside (1 M) was added, and the reaction mixture was incubated at 37 °C for 15 minutes. The reaction was terminated by adding 1 mL of 0.1 N sodium carbonate, and the absorbance was recorded at 405 nm. 50% DMSO served as a control, and acarbose was employed as the normal medication.

Percent inhibition of α-glucosidase activity was

determined using the following formula:

$$Inhibition(\%) = [\frac{(Ac - At)}{Ac}] \times 100$$

where Ac = absorbance of the control reaction mixture, At = absorbance of the test

**3.2.6. Anticancer Studies**

**3.2.6.1. Cells and Culture Conditions**

Human cancer cell lines, including glioma (U87MG), lung adenocarcinoma (A549), and breast carcinoma (MCF-7), were maintained in Dulbecco's Modified Eagle's Medium (DMEM) supplemented with 10% fetal bovine serum, 1% antibiotic-antimycotic solution, and 1% L-glutamine. The cells were incubated at 37 °C in a humidified atmosphere containing 5% $CO_2$, subcultured once they reached about 70% confluence, and utilized for experiments after three successive passages.

**3.2.6.2. Cytotoxicity assessment using Methyl Thiazolyl Tetrazolium (MTT) assay**

The cytotoxic effects of the test compounds against U87MG, MCF-7, and A549 cells were assessed using the MTT assay (Mosmann,1983). Cells were plated in 96-well plates at a density of 5,000 cells per well and allowed to adhere for 24 h at 37 °C in a humidified 5% $CO_2$ atmosphere. The test compounds were then applied at concentrations of 10, 25, 50, 100, and 250 µg/mL, and for an additional 48 h, the cells were incubated. The treatment, 100 µL of MTT solution (1 mg/mL), was added to each well and incubated for 3 h. The formed formazan crystals were dissolved in DMSO, and at 570 nm absorbance was taken using a multimode microplate reader (FluoSTAR Omega, BMG Labtech).

**3.2.6.3. Apoptosis detection using acridine orange-ethidium bromide (AO-EB) dual fluorescence staining**

U87MG, MCF-7, and A549 cells (10000 cells/well) were seeded onto 24-well surface-treated plates and incubated in complete DMEM at 37 ºC under 5% $CO_2$ in a humidified atmosphere for 24 h. Post-adherence, they were added with the $IC_{50}$ of the compounds **2b** and **4a**, and incubated under the same conditions for 48 h. Cells were stained using a 1:1 mixture of AO and EB (2 µg/mL) for 20 min in the dark at 37 ºC. The staining solution was removed, excess stain was washed with 1X PBS, and cells were overlaid with PBS. Nuclei were imaged under the green and red channels of a fluorescence imager (Zoe, BioRad) at 20X magnification.

**3.3. Molecular docking studies**

The EGFR kinase domain complexed with a quinazoline inhibitor (PDB: 1XKK)[36], the crystal structure of NS5 bound to the N-terminal bromodomain of BRD2 (PDB: 6JKE)[37] and the human estrogen receptor α-ligand-binding domain complexed with 4hydroxytamoxifen (PDB: 3ERT)[38] were retrieved from the Protein Data Bank (www.rcsb.org). Prior to protein preparation, all co-crystallized inhibitors, ligands, and water molecules were removed to obtain a clean protein structure. Subsequently, polar hydrogen atoms along with Gasteiger-Huckel charges were added to the protein before performing the docking studies [39] [40]. For molecular docking studies, grid parameters were defined based on the active site of each target protein. In the case of PDB ID: 1XKK, the grid box was generated with its center positioned at coordinates (78, 52, 72) and dimensions of 18.214 Å × 34.599 Å × 37.950 Å along the x, y, and z axes, respectively. For PDB ID: 6JKE, the grid center was set at (56, 46, 42), with grid dimensions of 14.599 Å, 10.543 Å, and 55.493 Å in the x, y, and z directions, respectively. Similarly, the grid box for PDB ID: 3ERT was centered at coordinates (76, 50, 86) with dimensions of 31.725 Å, −0.488 Å, and 19.496 Å along the respective axes.The chemical structures of the synthesized compounds were initially sketched using ChemDraw software. These structures were subsequently converted into three-dimensional conformations and subjected to energy minimization to obtain the most stable geometry prior to docking. Ligand preparation was carried out using AutoDock 4.2, where Gasteiger charges were assigned, nonpolar hydrogen atoms were merged, and rotatable bonds were defined. The prepared ligands were then docked into the binding pockets of the selected target proteins using AutoDock Vina. The binding affinities and molecular interactions of the docked complexes were finally examined and visualized with Discovery Studio software [41].

## 4. CONCLUSION

From this study, Thiazolopyrimidine-6-carboxylate and thiazole-pyrimidine-6-carbonitrile derivatives were successfully synthesized using the Biginelli reaction under solvent-free conditions and characterized by FTIR, $^1$H-NMR, $^{13}$C-NMR, and LC-MS. The biological studies showed that compound **4a** consistently displayed strong antibacterial, antioxidant, and anti-inflammatory activities, with results close to standard drugs. Compound **4e** showed the best activity in α-amylase and α-glucosidase inhibition assays, indicating good antidiabetic potential. Overall, the 4-series compounds, especially **4a** and **4e**, demonstrated promising biological activities and could be considered for further development as multi-functional drug candidates. Compound **4a** showed potential anticancer activity against lung cancer, breast cancer, and glioma cells, suggesting its promising role as a chemotherapeutic agent after appropriate validations.

**Acknowledgments**

Dr. Vinuta Kamat is thankful to Dayananda Sagar College of Engineering, Bangalore. The authors are grateful to the M. S. Ramaiah Institute of Technology, Bengaluru 560054, Karnataka, India, under the SEED money projects: MSRIT/Admin/1574/23-24.

**Conflicts of Interest**

There are no conflicts of interest to declare.

**References**


1. M. Abdel-Megid, K. M. El-Mahdy, A. M. Elkazak, S. E. Zarif and M. E. Salem, Synthetic approaches and biological evaluation of nitrogen bridgehead thiazolo [3, 2-a] pyrimidines. *Results Chem.* 11 (2024): 101807. https://doi.org/10.1016/j.rechem.2024.101807
2. B. V. Kendre, S. R. Bhusare and P. S. Hardas, Antimicrobial and anti-inflammatory activity studies of novel thiazolopyrimidines. *Asian J. Pharm. Res.* 10 (2020): 55-73. https://doi.org/10.46624/ajptr.2020.v10.i1.006
3. A. S. Abdelkhalek, M. S. Attia and M. A. Kamal, Triazolopyrimidine Derivatives: An Updated Review on Recent Advances in Synthesis, Biological Activities and Drug Delivery Aspects. *Curr. Med. Chem.* 31.14 (2024): 1896-1919. https://doi.org/10.2174/0929867330666230228120416
4. L. H. Al-Wahaibi, M. H. Abdel-Rahman, K. El-Adl, B. G. M. Youssif, S. Bräse and S. A. Abdel-Aziz, New Diaryl-1,2,4-triazolo[3,4-a]pyrimidine Hybrids as Selective COX-2/sEH Dual Inhibitors with Potent Analgesic/Anti-inflammatory and Cardioprotective Properties. *ACS Omega* 9.31 (2024): 33494-33509. https://doi.org/10.1021/acsomega.4c00870
5. M. R. Islam and H. Fahmy, Thiazolopyrimidine Scaffold as a Promising Nucleus for Developing Anticancer Drugs: A Review Conducted in Last Decade. *Anticancer Agents Med. Chem.* 22 (2022): 2942–2955. https://doi.org/10.2174/1871520622666220411110528
6. A. A. Abu-Hashem, M. M. Youssef and H. A. Hussein, Synthesis, antioxidant, antituomer activities of some new thiazolopyrimidines, pyrrolothiazolopyrimidines and triazolopyrrolothiazolopyrimidines derivatives. *J. Chin. Chem. Soc.* 58 (2011): 41–48. https://doi.org/10.1002/jccs.201190056
7. E. M. Flefel, W. A. El-Sayed, A. M. Mohamed, W. I. El-Sofany and H. M. Awad, Synthesis and anticancer activity of new 1-thia-4-azaspiro [4.5] decane, their derived thiazolopyrimidine and 1, 3, 4-thiadiazole thioglycosides. *Molecules* 22.1 (2017): 170. https://doi.org/10.3390/molecules22010170
8. M. S. Nazir, S. Aslam, M. Ahmad and A. F. Zahoor, Recent updates on the synthesis of thiazolopyrimidines derivatives. *Synth. Commun.* 2023, 53, 1173–1206. https://doi.org/10.1080/00397911.2023.2212096
9. M. N. Yousif, W. A. El-Sayed, H.-A. S. Abbas, H. M. Awad and N. M. Yousif, Anticancer activity of new substituted pyrimidines, their thioglycosides and thiazolopyrimidine derivatives. *J. Appl. Pharm. Sci.* 7.11 (2017): 021-032. https://dx.doi.org/10.7324/japs.2017.71104
10. S. H. Ali and A. R. Sayed, Review of the synthesis and biological activity of thiazoles. *Synth. Commun.* 51.5 (2021): 670-700. https://doi.org/10.1080/00397911.2020.1854787
11. K. Rajagopal, S. Dhandayutham, M. Nandhagopal, M. Narayanasamy, M. I. Elzagheid, L. Rhyman and P. Ramasami, Thiazole derivatives: Synthesis, characterization, biological and DFT studies. *J. Mol. Struct.* 1255 (2022): 132374. https://doi.org/10.1016/j.molstruc.2022.132374
12. V. R. Rao and V. R. Reddy, Silicon, Heterocyclic systems containing a bridge head nitrogen atom: Reaction of 5-pyrimidine carboxylic acid 1, 2, 3, 4-tetrahydro-6-methyl-4-aryl-2-thioxoethyl ester with 3-(2-bromoacetyl) coumarins. *Phosphorus Sulfur Silicon Relat. Elem.* 181.1 (2006): 147-158. https://doi.org/10.1080/104265090969252
13. S. Singh, A. Schober, M. Gebinoga and G. A. Groß, Convenient method for synthesis of thiazolo [3, 2-a] pyrimidine derivatives in a one-pot procedure. *Tetrahedron Lett.* 52.29 (2011): 3814-3817. https://doi.org/10.1016/j.tetlet.2011.05.067
14. I. Kulakov, O. Nurkenov, D. Turdybekov, G. Issabaeva, A. Mahmutova and K. Turdybekov, Synthesis of thiazolo [3, 2-a] pyrimidines based on 4-aryl-substituted 3, 4-dihydro-pyrimidine (1H)-2-thiones and the crystal structure of ethyl 5-(2, 4-dimethoxyphenyl)-7-methyl-3-oxo-3, 5-dihydro-2H-thiazolo-[3, 2-a] pyrimidine-6-carboxylate. *Chem. Heterocycl. Compd.* 45.7 (2009): 856-859.
15. O. Alam, S. A. Khan, N. Siddiqui, W. Ahsan, S. P. Verma and S. Gilani, Antihypertensive activity of newer 1, 4-dihydro-5-pyrimidine carboxamides: Synthesis and pharmacological evaluation. *Eur. J. Med. Chem.* 45.11 (2010): 5113-5119. https://doi.org/10.1016/j.ejmech.2010.08.022
16. H. H. Sayed, E. M. Morsy and E. R. Kotb, Facile novel synthesis and reactions of thiazolidin-4-one derivatives for antimicrobial agents. *Synth. Commun.* 40.18 (2010): 2712-2722. https://doi.org/10.1080/00397910903318674
17. S. F. Mohamed, E. M. Flefel, A. E.-G. E. Amr and D. N. Abd El-Shafy, Anti-HSV-1 activity and mechanism of action of some new synthesized substituted pyrimidine, thiopyrimidine and thiazolopyrimidine derivatives. *Eur. J. Med. Chem.* 45.4 (2010): 1494-1501. https://doi.org/10.1016/j.ejmech.2009.12.057
18. E. Korkusuz, Y. Sert, S. Arslan, H. Aydın, İ. Yıldırım, Y. Demir, İ. Gülçin and İ. Koca, Synthesis and biological studies of pyrimidine derivatives targeting metabolic enzymes. *Arch. Pharm.* 357.8 (2024): 2300634. https://doi.org/10.1002/ardp.202300634
19. M. Chalabi-Dchar, T. Fenouil, C. Machon, A. Vincent, F. Catez, V. Marcel, H. C. Mertani, J. C. Saurin, P. Bouvet, J. Guitton, N. D. Venezia and J. J. Diaz, A novel view on an old drug, 5-fluorouracil: an unexpected RNA modifier with intriguing impact on

cancer cell fate. *NAR Cancer* 3.3 (2021): zcab032. https://doi.org/10.1093/narcan/zcab032
20. J. Guo, Z. Xie, W. Ruan, Q. Tang, D. Qiao and W. Zhu, Thiazole-based analogues as potential antibacterial agents against methicillin-resistant *Staphylococcus aureus* (MRSA) and their SAR elucidation. *Eur. J. Med. Chem.* 2023, 259, 115689. https://doi.org/10.1016/j.ejmech.2023.115689
21. D. H. Dawood, D. O. Saleh, G. A. Abdel Jaleel and E. S. Nossier, New Chromone-Thiazolopyrimidine Hybrids as Potent TNF-α, IL-6 and PGE2 Inhibitors: Synthesis, Anti-Inflammatory Evaluation and Molecular Modeling Studies. *Polycycl. Aromat. Compd.* 2024, 44, 6564–6588. https://doi.org/10.1080/10406638.2023.2278668
22. S. Aggarwal, M. Devgun, R. Narang, S. Khokra, A. C. Rana and M. R. Goyal, Thiazolopyrimidines: A Retrospective Study of Synthesis, Structure-Activity Relationship and Diverse Pharmacological Actions. *Asian J. Chem.* 2022, 34, 519–530.
23. B. Kuppast and H. Fahmy, Thiazolo[4,5-d]pyrimidines as a privileged scaffold in drug discovery. *Eur. J. Med. Chem.* 113 (2016): 198-213. https://doi.org/10.1016/j.ejmech.2016.02.031
24. D. Gjorgieva Ackova, J. Kotur-Stevuljevic, C. Bhushan Mishra, P. Mehta Luthra and L. Saso, Antioxidant properties of synthesized bicyclic thiazolopyrimidine derivatives as possible therapeutic agents. *Antioxidants* 9 (2018): 113. https://doi.org/10.3390/app9010113
25. M. Tolba, M. Sayed, A. Abdel-Raheem Sh., T. Gaber, A. Kamal El-Dean and M. Ahmed, Synthesis and spectral characterization of some new thiazolopyrimidine derivatives. *Chem. Chem. Lett.* 2021, 10, 471–478.
26. K. I. Kaskevich, A. A. Babushkina, V. V. Gurzhiy, D. M. Egorov, N. I. Svintsitskaya and A. V. Dogadina, Synthesis of 3 (2)-phosphonylated thiazolo [3, 2-a] oxopyrimidines. *Beilstein J. Org. Chem.* 16 (2020): 1947-1954. https://doi.org/10.3762/bjoc.16.161
27. S. Y. Ewieda, M. M. Salem, A. Elshewy, M. Abdalla, M. El-Manawaty, H. K. Abdelhady, H. H. Haredy, W. A. Fadaly, M. F. Mohamed and M. T. Nemr, Discovery of novel thiazolopyrimidine derivatives targeting topoisomerase II: Design, synthesis, antiproliferative evaluation, molecular docking and apoptosis inducing activity. *Bioorg. Chem.* (2025): 108672. https://doi.org/10.1016/j.bioorg.2025.108672
28. S. Aggarwal, M. Devgun, R. Narang, S. Lal, A. Rana and R. Goyal, Thiazolopyrimidines: A Retrospective Study of Synthesis, Structure-Activity Relationship and Diverse Pharmacological Actions. *Asian J. Chem.* 34 (2022): 519-530.
29. F. Mohamadpour, Environmentally Friendly and Facile Synthesis of 2-oxo-and Thioxo-1, 2, 3, 4-tetrahydropyrimidines Catalyzed by Formic Acid as a Natural Green and Bio-based Catalyst under Solvent-Free Conditions. *Curr. Med. Chem.* 19 (2020): 61-75. https://doi.org/10.12982/CMUJNS.2020.0005
30. M. A. Al-Omar, A.-R. M. Al-Obaid, N. R. El-Brollosy and A. A. El-Emam, Some observations on the base-catalyzed cyclocondensation of 2, 6-dihalobenzaldehydes, ethyl cyanoacetate, and thiourea. *Synth. Commun.* 40 (2010): 1530-1538. https://doi.org/10.1080/00397910903098730
31. R. M. Humphries, J. Ambler, S. L. Mitchell, M. Castanheira, T. Dingle, J. A. Hindler, L. Koeth and K. M. Sei, CLSI methods development and standardization working group best practices for evaluation of antimicrobial susceptibility tests. *J. Clin. Microbiol.* 56 (2018): 10.1128/jcm.01934-01917. https://doi.org/10.1128/jcm.01934-17
32. W. Brand-Williams, M. E. Cuvelier and C. Berset, Use of a free radical method to evaluate antioxidant activity. *Food Sci. Technol.* 28 (1999): 1231-1237.
33. E. M. Altundag, D. Gençalp, C. Özbilenler, K. Toprak and N. Kerküklü, In vitro antioxidant, anti-inflammatory and anti-cancer activities of methanolic extract of *Asparagus horridus* grows in North Cyprus. *Turk. J. Biochem.* 45 (2020): 365-372. https://doi.org/10.1515/tjb-2019-0325
34. N. Boechat, V. F. Ferreira, S. B. Ferreira, M. L. G. Ferreira, F. C. Silva, M. M. Bastos, M. S. Costa, M. C. S. Lourenço, A. C. Pinto and A. U. Krettli, Novel 1,2,3-triazole derivatives for use against *Mycobacterium tuberculosis* H37Rv (ATCC 27294) strain. *J. Med. Chem.* 54 (2011): 5988-5999. https://doi.org/10.1021/jm2003624
35. Kamat, D. A. Barretto, B. Poojary, A. Kumar, V. B. Patil and S. Hamzad, In vitro α-amylase and α-glucosidase inhibition study of dihydropyrimidinones synthesized via one-pot Biginelli reaction in the presence of a green catalyst. *Bioorg. Chem.* 143 (2024): 107085. https://doi.org/10.1016/j.bioorg.2023.107085
36. E. R. Wood, A. T. Truesdale, O. B. McDonald, D. Yuan, A. Hassell, S. H. Dickerson, B. Ellis, C. Pennisi, E. Horne and K. Lackey, A unique structure for epidermal growth factor receptor bound to GW572016 (Lapatinib) relationships among protein conformation, inhibitor off-rate, and receptor activity in tumor cells. *Cancer Res.* 64 (2004): 6652-6659. https://doi.org/10.1158/0008-5472.CAN-04-1168
37. P. Deshmukh, S. Mathur, G. Gangadharan, G. Krishnappa, N. D. Nanjaiah and B. Padmanabhan, Novel pyrano 1,3 oxazine based ligand inhibits the epigenetic reader hBRD2 in glioblastoma. *Biochem. J.* 477 (2020): 2263-2279. https://doi.org/10.1042/BCJ20200339
38. A. K. Shiau, D. Barstad, P. M. Loria, L. Cheng, P. J. Kushner, D. A. Agard and G. L. Greene, The structural basis of estrogen receptor/coactivator recognition and the antagonism of this interaction by tamoxifen. *Cell* 95 (1998): 927-937. https://doi.org/10.1016/S0092-8674(00)81717-1

39. B. Kallauraya, R. S. Bhat, S. I. Bhat, V. Kamat, M. Akki, A. Kumar, K. Jyothi and B. Bharat, Synthesis, characterization, and evaluation of pyrimidinone-linked thiazoles: DFT analysis, molecular docking, corrosion inhibition, and bioactivity studies. *Heliyon* 2024, 10.
40. Babagond, K. Katagi, M. Akki, D. S. Reddy, H. Shanavaz, A. Jaggal and S. D. K., Design and synthesis of potent anticancer agents using coumarin-quinazolinone based scaffolds: exploration of ADME properties and molecular docking studies. *ChemistrySelect* 9 (2024): e202400435. https://doi.org/10.1002/slct.202400435
41. O. Trott and A. J. Olson, AutoDock Vina: improving the speed and accuracy of docking with a new scoring function, efficient optimization, and multithreading. *J. Comput. Chem.* 31 (2010): 455-461. https://doi.org/10.1016/j.rechem.2024.101807